

Triple-Stranded Metallo-Helicates Addressable as Lloyd's Electron Spin Qubits

Yasushi Morita,^{*,†,§} Yumi Yakiyama,[†] Shigeaki Nakazawa,^{‡,§} Tsuyoshi Murata,[†] Tomoaki Ise,^{‡,§}
Daisuke Hashizume,[†] Daisuke Shiomi,^{‡,§} Kazunobu Sato,^{‡,§} Masahiro Kitagawa,^{||,§}
Kazuhiro Nakasuji,[†] and Takeji Takui^{*,‡,§}

Department of Chemistry, Graduate School of Science, Osaka University, Toyonaka, Osaka 560-0043, Japan, CREST, Japan Science and Technology (JST), Chiyoda-ku, Tokyo 102-0075, Japan, Departments of Chemistry and Materials Science, Graduate School of Science, Osaka City University, Sumiyoshi-ku, Osaka 558-8585, Japan, Advanced Technology Support Division, RIKEN, Wako-shi, Saitama 351-0198, Japan, and Graduate School of Engineering Science, Osaka University, Toyonaka, Osaka 560-8531, Japan

Received March 10, 2010; E-mail: morita@chem.sci.osaka-u.ac.jp; takui@sci.osaka-cu.ac.jp

Quantum computers (QCs) and quantum information processing systems (QIPSs) are rapidly emerging in pure and applied sciences.¹ The past few years have witnessed that the implementation of QCs/QIPSs has become the focus of current topics in chemistry.^{2,3} Building-up scalable quantum bits (qubits) in a controlled manner is the most intractable issue to be solved for any physical system pursuing realistic practical QCs/QIPSs. Thus, implementation of scalable matter qubits is now a materials challenge for scientists from an experimental approach.³ Among matter qubits, molecular electron spin qubits can afford promise in implementing scalable QCs/QIPSs, as relevant to an electron spin-qubit version of a Lloyd (ABC)_n model.⁴ Lloyd's proposal gives an alternative practical approach to scalable QCs instead of implementing a vast number of addressable qubits. Lloyd's models of electron spin qubits require spatial alignment of open-shell entities with nonequivalent *g*-tensors in appropriately designed molecular frames (termed *g*-tensor engineering).^{3c} However, any experimental reports of Lloyd's system have never been presented.

An imidazole-ring system is a useful building block as a well-ordered structure featuring two-directional coordination and/or hydrogen bonds (H-bonds). Oligo(imidazole)s, as shown in Figure 1, have 4,4'-biimidazole moieties (Figure 1, *n* = 0: **Bim**), which are bidentate ligands capable of multidimensional networks.⁵ In this study, we have for the first time implemented the *g*-tensor molecular engineering by the use of newly designed triple-stranded metallo-helicates of an imidazole tetramer, quaterimidazole (Figure 1, *n* = 1: **Qim**) with Mn(II) or Zn(II) cations (Figures S1–8, Tables S1–2).⁶ This study links supramolecular chemistry to the field of QCs/QIPSs and gives a prototype of synthetic electron spin qubits of the formidable Lloyd model.

Our basic concept for electron spin-qubit versions of a Lloyd model, i.e. *g*-tensor engineering, is shown in Figure 1. Oligo(imidazole)s, with *n* > 0, can afford to form multinuclear helicates (space filling model in Figure 1).⁶ In such helicates, each open-shell metal ion carrying electron-spin qubits is magnetically nonequivalent because of the twisted helical structure formation with the pseudo-octahedral coordination environments around them in the crystalline states. This structural salient feature of oligo(imidazole)s-based helicates gives us nonequivalent *g*-tensor systems. Noticeably, in the triple-stranded trinuclear helicates, the two outermost open-shell ion sites give two nonequivalent *g*-tensors differing from that

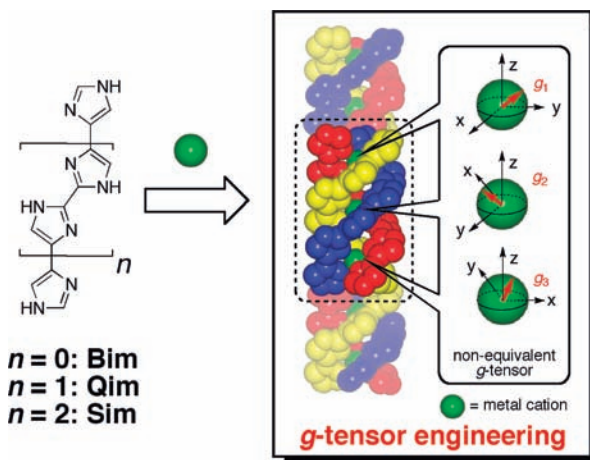


Figure 1. Basic concept for *g*-tensor engineering with electron-spin in oligo(imidazole)s-based triple helicates for an electron spin-qubit version of the Lloyd model. Oligo(imidazole) molecules form a triple-stranded helicate with nonequivalent *g*-tensors (space filling model); central deep colored trinuclear helicate is composed of **Sim** (*n* = 2).

of the central ion. Noteworthy, in a trinuclear triple helicate including lanthanide cations in solution, the difference in magnetic environments has been shown with the help of paramagnetic NMR measurements.⁸ This gives rise to the (ABC) electron spin-qubit model for the 1D periodic Lloyd system. To achieve selective spin excitations for QC (Quantum Computing) processing under currently available pulse microwave technology, further conditioning, i.e. weakening intra- and interhelicate exchange interactions, is essential.^{3,9} In the 1D (ABC)_n periodic model systems for QCs/QIPSs, it is a requisite that intrahelicate exchange interactions between the spin-bearing cations are weak and interhelicate ones are vanishing. The former is required for executing quantum operations under current restrictions of pulse microwave technology, and the latter for suppressing decoherence effects on the qubits during the operation. Open-shell metal cations within the helicate scaffold have to maintain sufficient distance for weakening the exchange interactions. As for vanishing interhelicate metal...metal exchange interactions, we have adopted magnetically diluted single crystals, in which guest ions carrying electron-spin qubits are embedded in diamagnetic host crystal lattices, truncating the interhelicate metal...metal interactions.

Magnetically diluted mixed single crystals of [Mn₂(**Qim**)₃](NO₃)₄/[Zn₂(**Qim**)₃](NO₃)₄ were grown from the cocrystallization of Mn(II)-centered guest and Zn(II)-centered host helicates in various

[†] Graduate School of Science, Osaka University.

[‡] Graduate School of Science, Osaka City University.

[§] CREST, JST.

^{||} Graduate School of Engineering Science, Osaka University.

^{*} Riken.

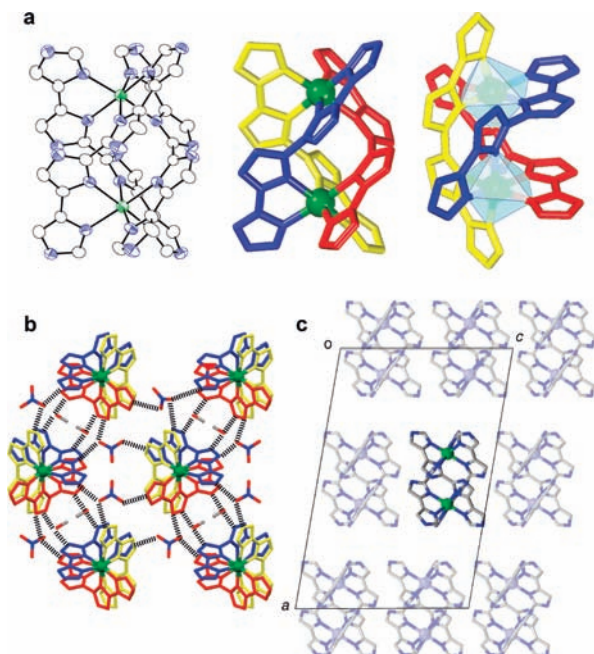


Figure 2. Crystal structure of the magnetically diluted crystal system of $[\text{Mn}_2(\text{Qim})_3](\text{NO}_3)_4/[\text{Zn}_2(\text{Qim})_3](\text{NO}_3)_4$. (a) Triple-stranded helical structure of $[\text{M}_2(\text{Qim})_3](\text{NO}_3)_4$ ($\text{M} = \text{Mn}(\text{II})$ or $\text{Zn}(\text{II})$). Left: ORTEP view at 50% probability level. Center: A stick model. Right: A stick model with two different pseudo-octahedral environments around metal ions. Only right-handed isomers are shown. H atoms and NO_3^- anions are omitted for clarity. (b) 2D sheet structure of $[\text{M}_2(\text{Qim})_3](\text{NO}_3)_4$ viewed along the a^* axis. (c) Image picture of the magnetically diluted crystal system. In the crystal, $\text{Zn}(\text{II})$ -centered helicites (light color) are isostructurally substituted by $\text{Mn}(\text{II})$ -centered guest helicites (deep color) at an elaborate concentration.

mixing ratios in $\text{MeOH}/\text{CHCl}_3$ at ambient temperature. X-ray structural analyses revealed that the diluted crystals crystallized in the monoclinic system with space group $C2/c$. In the crystal, right- and left-handed dinuclear triple helicites with pseudo-octahedral coordination geometry were formed. The two metal ions embedded in a helicate maintaining a relatively long distance ($>5 \text{ \AA}$) were related by 2-fold helical symmetry, leading to two nonequivalent g -tensors at the two $\text{Mn}(\text{II})$ sites with a weak $\text{Mn}(\text{II}) \cdots \text{Mn}(\text{II})$ exchange coupling (Figure 2, Figures S9–10 and Table S3). It is noteworthy that the $C2/c$ space group crystal has three kinds of symmetry elements, inversion, translation, and rotation. In our crystal, inverted and translationally related metal ions are magnetically equivalent, giving “magnetically only one kind of helicate in a unit cell.” Consequently, the targeted g -tensor engineering to design two addressable electron spin qubits has successfully been achieved. This information, together with the pseudo-octahedral symmetry elaborately made, is of essential importance in ESR measurements, as described later.

The cell parameter of the diluted single crystal was the same as that of the $[\text{Zn}_2(\text{Qim})_3]^{4+}$ host single crystal, and thus as predicted, the crystal structure and alignment of components in the diluted crystal were the same as those of the host $\text{Zn}(\text{II})$ crystal (Figures S3–4, S9–10, Tables S2–3). This tendency was kept constant with changes of the $\text{Mn}(\text{II})/\text{Zn}(\text{II})$ ratio. This is one of the advantages of the helicites under study for designing scalable matter spin qubits. The successful formation of the diluted crystal is due to the high stability of oligo(imidazole)s-based helicites in solution ($K = 10^{19} - 10^{20} \text{ M}^{-4}$), as proven by ESI-MS and UV spectra (Figures S5–8).⁶ It also should be noted that the outward H-bonding sites having the same interaction modes of both $\text{Zn}(\text{II})$ host and $\text{Mn}(\text{II})$ guest helicites enable the preparation of the diluted crystals in

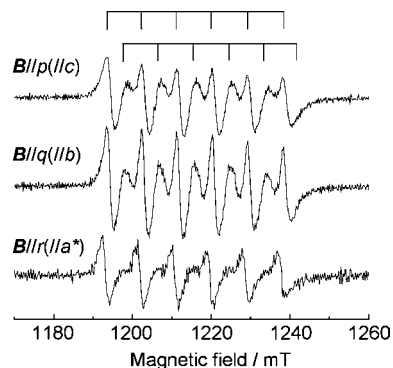


Figure 3. Q-band ESR spectra of the magnetically diluted crystal of $[\text{Mn}_2(\text{Qim})_3](\text{NO}_3)_4/[\text{Zn}_2(\text{Qim})_3](\text{NO}_3)_4$ ($\text{Mn}(\text{II})/\text{Zn}(\text{II}) = 1:10$) observed at 15 K. The magnetic field \mathbf{B} was oriented along the $p//c$ (top), $q//b$ (middle), and $r//a^*$ (bottom) axis. Broadened hyperfine lines attributed to the two $\text{Mn}(\text{II})$ nuclei ($I = 5/2$) are resolution-enhanced by invoking the subtraction of the second derivative component for each line.¹² Frequency used was 34.05407, 34.04936, and 34.01984 GHz for $\mathbf{B}//p$, $\mathbf{B}//q$, and $\mathbf{B}//r$. The S/N ratio of the spectrum depends on the resonator Q-value governed by the orientation.

various mixing ratios (Figure S11, Tables S1–3). Such H-bonding ability is exceedingly rare in helicate chemistry.¹⁰ As a result, the $\text{Mn}(\text{II})$ -centered helicites were isostructurally replaced and diluted in the $\text{Zn}(\text{II})$ helicate lattices at a desired concentration in the diluted crystal. This H-bond-driven replacement method serves as a new approach to prepare diluted crystals for metallo-complexes.

On the basis of these structural data, we have characterized the spin addressability of the oligo(imidazole)s-based helicites embedding open-shell $\text{Mn}(\text{II})$ cations as matter spin qubits, particularly focusing on whether they undergo the g -tensor engineering along with desired weak exchange interactions between the cations. The single-crystal ESR spectroscopy at the Q-band, which gives a three times higher g -resolution than the X-band, has illustrated the occurrence of the targeted g -engineering. In Figure 3, a pair of six-line resolved hyperfine structures are observed with the static magnetic field along the crystallographic axes, $a^*//r$, $b//q$, and $c//p$, where the a^* axis is perpendicular to the b and c axes (Figure S12). Each six-line hyperfine structure with a different g -value is attributed to the $\text{Mn}(\text{II})$ nuclear hyperfine allowed ESR transitions between the electron spin sublevels $M_S = +1/2$ and $-1/2$ in the sextet state ($S = 5/2$) of pseudo-octahedral symmetry. Because of the $C2/c$ helical symmetry, the two kinds of the hyperfine structure arise from the two $\text{Mn}(\text{II})$ nuclei embedded within one helicate. A pair of the six-line hyperfine splitting were angular-dependent on the static magnetic field in the crystal graphic axes reference, giving two kinds of the g -tensors with small anisotropy.

The experimental principal values for the g -tensors are $\mathbf{g}_1 = (g_1, g_2, g_3) = (2.00524, 2.00466, 2.00404)$ and $\mathbf{g}_2 = (2.00073, 2.00041, 1.99984)$ (Table S4). A typical standard deviation for the g -values is ± 0.0008 . The principal axis of g_3 for both \mathbf{g}_1 and \mathbf{g}_2 lies along the direction connecting the two $\text{Mn}(\text{II})$ nuclei in the helicate. The hyperfine splitting due to the $\text{Mn}(\text{II})$ nuclei are isotropic ($a_{\text{iso}}^{\text{Mn}} = 8.96 \text{ mT}$) within experimental error. It is noteworthy that a pair of the $\text{Mn}(\text{II})$ hyperfine structure with the isotropic hyperfine constant and their angular dependence due to the small g -anisotropy reasonably agree with the salient features of the X-ray analyzed crystal structure, indicating that the targeted g -tensor engineering to design two electron spin-qubit molecular systems has successfully been achieved. The anisotropic contribution of the fine structure to the hyperfine allowed ESR transitions between $M_S = +1/2$ and $-1/2$ vanishes to the first order for odd-integral spins. Thus, the observed anisotropy of the hyperfine

structure is attributable to the g -anisotropy of the Mn(II) ion embedded in the helicate.¹¹ The temperature dependence of $\chi_p T$ derived from SQUID measurements on $[\text{Mn}_2(\mathbf{Qim})_3]^{4+}$ in the crystalline state obeyed a simple Curie–Weiss behavior with $\theta = -0.14$ K (θ : Weiss constant), giving a g -value of 1.99 with $S = 5/2$ (Figure S13). These results indicated that there are only weak but detectable exchange interactions between the helicates in the bulk ensemble, being consistent with the X-ray crystal structure data.

To illustrate, from another viewpoint, that the molecular g -engineering for matter spin qubits is achieved in our helicates, we have carried out state-of-the-art quantum chemical calculations¹³ to characterize the g -tensors of the open-shell metal sites, focusing on the departure from octahedral symmetry at the Mn(II) site in terms of the g -tensor (Tables S5–6). The degree of the g -anisotropy is essential for the currently available pulse microwave technology for implementing QC/QIP, in which electron spin qubits are selectively excited during quantum gate operations. This situation contrasts with the NMR paradigm in implementing QC/QIP. The quantum chemical calculations for the Mn(II) site based on the X-ray-determined structures showed that the g -tensors are of rhombic nature ($g_1^{\text{calc}} = 2.00135$, $g_2^{\text{calc}} = 2.00156$, $g_3^{\text{calc}} = 2.00157$); the principal axis for g_1^{calc} is along the Mn···Mn direction, which corresponds to the g_3 axis determined from the experiment, reasonably being consistent with the observed g -anisotropy. The agreement indicates that the twisted helical symmetry formation achieved in the helicates is capable of subtle molecular g -tensor engineering for (ABC)-based 1D electron spin-qubit arrays.

In conclusion, we have for the first time illustrated the molecular design that can afford an electron-spin-based Lloyd model⁴ for scalable matter spin qubits by invoking newly designed triple-stranded helicates embedding open-shell metal ions in a one-dimensional manner.⁶ The key to successful molecular design is introduction of oligo(imidazole)s ligands to self-organize metal ions in a controlled manner. Oligo(imidazole)s-based helicates possess a high metal-recognition ability, packing controllability based on outward H-bonds, and above all synthetic scalability as matter spin qubits.¹⁴ This “universality” of oligo(imidazole)s-based triple helicates enable us to increment the number of the addressable qubits by embedding other metal ions, extending the helicate length with longer oligomers such as **Sim** and finely tuning inter- and intrahelicate exchange interactions.¹⁴ The helical chirality can also be a good tool for linking matter spin qubits with photon qubits.¹⁵ QC experiments with the use of high-power Q-band pulse-based EElectron-electron-DOuble Resonance (ELDOR) are underway. This materials challenge closely related to innovation of pulse microwave electron spin technology can pave the road to the implementation of practical scalable electron spin qubits for QCs/QIPs.

Acknowledgment. This work was partly supported by grants of Ogasawara Foundation, Iketani Science and Technology Foundation, The Global COE program “Global Education and Research Center for Bio-Environmental Chemistry” of Osaka University, and

Grants-in-Aid from the Ministry of Education, Culture, Sports, Science and Technology, Japan. We thank Professor K. Hirose for fruitful discussions of the solution state behavior. Y.Y. is a recipient of Japan Society for the Promotion of Science (JSPS) research fellowship.

Supporting Information Available: Experimental details and ESI-MS, UV–vis, X-ray crystal analysis data and complete ref 3b and 3c. This material is available free of charge via the Internet at <http://pubs.acs.org>.

References

- (1) (a) Shor, P. W. *Proceedings, 35th Annual Symposium on Foundations of Computer Science*; IEEE Press: Los Alamitos, CA, 1994. (b) Sohn, L.; Kouwenhoven, L.; Schon, G. *Mesoscopic Electron Transport, NATO ASI Series E*; Kluwer Academic Publishers: Dordrecht, 1997. (c) Mehring, M.; Mende, J.; Scherer, W. *Phys. Rev. Lett.* **2003**, *90*, 153001. (d) Mehring, M.; Scherer, W.; Weidinger, A. *Phys. Rev. Lett.* **2004**, *93*, 206603. (e) Wang, H.; Nori, A. S. *Phys. Rev. A* **2009**, *79*, 042335.
- (2) (a) A thematic issue on “molecular spintronics and quantum computing” has recently been published in: *J. Mater. Chem.* **2009**, *19*, 1661–1768. (b) Kassal, I.; Aspuru-Guzik, A. *J. Chem. Phys.* **2009**, *131*, 224102. (c) Lanyon, B. P.; Whitfield, J. D.; Gillett, G. G.; Gogin, M. E.; Almeida, M. P.; Kassal, I.; Biamonte, J. D.; Mohseni, M.; Powell, B. J.; Brbieri, M. *Nature Chem.* **2010**, *2*, 106–111.
- (3) (a) Rahimi, R.; Sato, K.; Furukawa, K.; Toyota, K.; Shiomi, D.; Nakamura, T.; Kitagawa, M.; Takui, T. *Int. J. Quantum Inf.* **2005**, *3*, 197–204. (b) Sato, K.; et al. *Physica E* **2007**, *40*, 363–366. (c) Sato, K.; et al. *J. Mater. Chem.* **2009**, *19*, 3739–3754.
- (4) Lloyd, S. *Sci. Am.* **1995**, *73*, 140–145.
- (5) (a) Morita, Y.; Murata, T.; Yamada, S.; Tadokoro, M.; Ichimura, A.; Nakasuji, K. *J. Chem. Soc., Perkin Trans. 1* **2002**, 2598–2600. (b) Morita, Y.; Murata, T.; Fukui, K.; Tadokoro, M.; Sato, K.; Shiomi, D.; Takui, T.; Nakasuji, K. *Chem. Lett.* **2004**, *33*, 188–189. (c) Murata, T.; Morita, Y.; Fukui, K.; Yakiyama, Y.; Sato, K.; Shiomi, D.; Takui, T.; Nakasuji, K. *Cryst. Growth Des.* **2006**, *6*, 1043–1047. (d) Murata, T.; Morita, Y.; Yakiyama, Y.; Yamamoto, Y.; Yamada, S.; Nishimura, Y.; Nakasuji, K. *Cryst. Growth Des.* **2008**, *8*, 3058–3065.
- (6) Experimental evidence of the formations of triple-stranded dinuclear metallo-helicates⁷ of **Qim** with Mn(II) and Zn(II) in solution and solid states is described in the Supporting Information.
- (7) Metallo-helicate: a supramolecular metal complex having helical structure; see: (a) Lehn, J.-M. *Supramolecular Chemistry—Concepts and Perspectives*; VCH: Weinheim, 1995. (b) Piguet, C.; Bernardinelli, G.; Hopfgartner, G. *Chem. Rev.* **1997**, *97*, 2005–2062. (c) Albrecht, M. *Chem. Rev.* **2001**, *101*, 3457–3497.
- (8) Ouali, N.; Rivera, J.; Morgantini, P.; Weber, J.; Piguet, C. *Dalton Trans.* **2003**, 1251–1263.
- (9) Leuenberger, M.; Loss, D. *Nature* **2001**, *410*, 789–793.
- (10) O–H···O or O–H···Cl type hydrogen bonds connect helicates to construct one-dimensional chain structures. See: Lavalette, A.; Tuna, F.; Clarkson, G.; Alcock, N. W.; Hannon, M. J. *Chem. Commun.* **2003**, 2666–2667.
- (11) The observed hyperfine structure shows line-broadening effects attributable to the nonvanishing fine-structure tensors. The effects arise from the departure from complete octahedral symmetry at the Mn(II) sites; note that the complete symmetry with the sextet state gives only a single ESR fine-structure transition due to vanishing fine-structure parameters.
- (12) Poole, C. P., Jr. *Electron Spin Resonance: A Comprehensive Treatise on Experimental Techniques*; John Wiley & Sons: New York, 1967.
- (13) (a) te Velde, G.; Bickelhaupt, F. M.; Baerends, E. J.; Fonseca Guerra, C.; van Gisbergen, S. J. A.; Snijders, J. G.; Ziegler, T. *J. Comput. Chem.* **2001**, *22*, 931–967. (b) Schreckenbach, G.; Ziegler, T. *J. Phys. Chem. A* **1997**, *101*, 3388–3399.
- (14) Further studies on metallo-helicates with different metal centers and π -extended ligand **Sim** will be reported elsewhere.
- (15) Optical resolutions of the helicates of **Qim** have been achieved. Detailed experimental results will be published soon.

JA102030W